



HAL
open science

Understanding macromolecules formation from the catalytic hydroconversion of pyrolysis bio-oil model compounds

M. Ozagac, C. Bertino-Ghera, D. Uzio, M. Rivallan, D. Laurenti, C. Geantet

► **To cite this version:**

M. Ozagac, C. Bertino-Ghera, D. Uzio, M. Rivallan, D. Laurenti, et al.. Understanding macromolecules formation from the catalytic hydroconversion of pyrolysis bio-oil model compounds. *Biomass and Bioenergy*, 2016, 95, pp.182-193. 10.1016/j.biombioe.2016.10.007 . hal-01428620

HAL Id: hal-01428620

<https://hal.science/hal-01428620>

Submitted on 8 Mar 2023

HAL is a multi-disciplinary open access archive for the deposit and dissemination of scientific research documents, whether they are published or not. The documents may come from teaching and research institutions in France or abroad, or from public or private research centers.

L'archive ouverte pluridisciplinaire **HAL**, est destinée au dépôt et à la diffusion de documents scientifiques de niveau recherche, publiés ou non, émanant des établissements d'enseignement et de recherche français ou étrangers, des laboratoires publics ou privés.



Distributed under a Creative Commons Attribution - NonCommercial 4.0 International License

Understanding macromolecules formation from the catalytic hydroconversion of pyrolysis bio-oil model compounds

M. Ozagac^a, C. Bertino-Ghera^{a,*}, D. Uzio^a, M. Rivallan^a, D. Laurenti^b, C. Geantet^b

^a IFP Energies Nouvelles, Rond-point de l'échangeur de Solaize, BP3, 69360 Solaize, France

^b IRCELYON, UMR5256 CNRS-UCBL, 2 Avenue A. Einstein, 69626 Villeurbanne Cedex, France

Catalytic hydroconversion of pyrolysis bio-oils is a promising process that can greatly contribute to their deoxygenation. Other simultaneous reactions such as condensation or oligomerization leading to heavy molecular weight compounds are detrimental to the process and still not well understood. This study deals with the hydroconversion of D-glucose and furfural in a batch reactor with a NiMo/alumina catalyst. Considering the carbon balances and SEC-RI analysis of hydroconversion products, we describe fast reaction pathways leading to soluble macromolecules (up to 700 g mol⁻¹) that are further precipitated into the solid phase. From the D-glucose conversion, ¹³C NMR analysis of residues revealed significant amounts of aromatic carbons. Also detected by FTICR-MS analysis of a liquid effluent, those structures were likely formed through dehydration reactions. Finally, a high water content in the feed demonstrated that D-glucose was preserved from dehydration reactions contrary to furfural which is prone to be hydrolyzed into soluble macromolecules precursors.

1. Introduction

In order to meet the growing demand in transportation fuels and chemicals, lignocellulosic biomass could be used as a renewable and CO₂-neutral source. The most widely studied softwood feedstock are pine or spruce and cork or oak as regards hardwoods. Lignocellulose is commonly composed of three major fractions: 40–45 wt% of cellulose (dry composition), 25–35 wt% of hemicelluloses, 15–30 wt% of lignin and up to 10 wt% of other compounds (such as minerals). Flash pyrolysis is a thermochemical liquefaction process that can be used to transform solid biomass into liquid [1,2]. However, the pyrolysed bio-oils have limited end-user application due to the acidity, their low heat capacity (compared to fossil fuels), their immiscibility with fossil hydrocarbons and their thermal instability due to their high oxygen content. Oxygen is present in organic compounds but also as free water which can represent up to 30 wt% of the raw bio-oil. Since the last 30 years, many laboratories [3] have tried to perform upgrading process inspired from petroleum feedstock catalytic hydroconversion (HDC). However, upgrading biomass-derived oils from

flash pyrolysis to produce hydrocarbons requires a significant oxygen removal before any subsequent conventional refining process.

In parallel to the deoxygenation reactions, several literature studies [3,4] show the occurrence of competitive reactions such as polymerization, condensation or oligomerization which promote the production of solid residues. This phenomenon is detrimental to the process because it leads to severe plugging of the equipment and to the catalyst deactivation. The coking ability especially due to the bio-oils thermal instability is a process limitation and needs an in-depth comprehension prior to any industrial scaling-up. Venderbosch [4,5] and Elliott [6] published studies describing the competition between hydroconversion pathways and the formation of liquid soluble high molecular mass compounds (also called macromolecules). However, the involved reaction mechanisms are not fully depicted. So far, those soluble compounds are also poorly identified by currently available analytical techniques [7,8]. To get an insight of soluble macromolecules contained into upgraded pyrolysis oil, Hoekstra [9] and more recently Castellvi [10] used the size exclusion chromatography (SEC) to detect molecular weights up to 1000 g mol⁻¹ PS eq. (Polystyrene equivalent). Those compounds are also called “pyrolytic lignin”, which corresponds to the water insoluble fraction of bio-oils and exhibit a highly aromatic structure [11].

To get a better molecular insight, some studies attempted to use

* Corresponding author.

E-mail address: celine.bertino-ghera@ifpen.fr (C. Bertino-Ghera).

model molecules representative of bio-oils composition. The thermal degradation products of lignin are generally represented [1,12] by phenolic species such as guaiacol, anisole or phenol derivatives [13]. On the other hand, carbohydrates and furans derivatives are commonly used to represent compounds resulting from flash pyrolysis liquefaction of cellulose and hemicelluloses respectively [14].

Contrary to representative ex-lignin compounds, carbohydrates and their derivatives have not been extensively studied in HDC conditions. Levoglucosan [15,16] and D-glucose [17] are typically chosen as representative compounds. Even if levoglucosan is present in high amount in pyrolysis bio-oils, it is readily converted to D-glucose in hydroconversion conditions [16–18]. Thus, in this work, D-glucose was chosen as the cellulose-derivative model molecule.

At a molecular level, many works deal with the conversion of aqueous diluted D-glucose solutions [19–24]. They distinguished a catalytic pathway involving sorbitol and a thermal pathway to furanic species such as 5-(Hydroxymethyl)furfural (5-HMF). Girisuta et al. [25] observed the predominance of the pathway involving furans when organic acids were introduced in the feed and Wildshut [26] studied the D-glucose hydroconversion with Ru/C and Pd/C catalysts. However, none of them complies with the corresponding carbon balances or attempts to describe the macromolecules formed by condensation reactions also called “humins” referring to water-insoluble organic compounds in aquatic systems. Buffle [27] reviewed in detail studies about physical and chemical properties of “humins” and their precursors such as humic and fulvic acids. Kleinhempel [28] presented a 3D molecular modelling involving the polymorphic condensation of oxygenated aromatics, aliphatics, ketones, nitrogen groups and non-organic compounds (mineral and metal compounds). Nevertheless, comparison between such macromolecules and those produced during a sugar-like compound hydroconversion has never been investigated so far. In order to avoid the extensive formation of “humins”, the catalytic hydroconversion of sorbitol was studied [29]. Detected products were found to result not only from hydrogenation reactions but also from several parallel reactions such as dehydration, retro-aldol condensation or dehydrogenation followed by decarbonylation [30]. Macromolecules was assumed to arise from hydrated furans such as 2,5-dioxo-6-hydroxy-hexanal (reported as DHH) leading to macromolecular structures [31,32] through aldol condensations. More recently, Hu [33] compared the formation of soluble macromolecules during the catalytic hydroconversion of 5-HMF using water or methanol as a solvent. In this case, methanol reacted with acidic compounds (levulinic acid for instance) through esterification reactions which prevent undesirable pathways.

Furfural reactivity in hydroconversion process has been deeply investigated [34] as model molecule arising from hemicellulose flash pyrolysis [14]. Kubickova et al. [35] extensively reported furfural hydroconversion in presence of various catalytic active phases. By studying furfural hydroconversion between 210 and 250 °C with a Pd-based catalyst, decarbonylation and hydrogenation routes were also observed as the two main pathways by Sithisa et al. [36–38]. The decarbonylation reaction needs higher activation energy than hydrogenation reaction which, explains its predominance at higher temperature. In addition, furfural was also studied as precursors for resins production. Identified reactions were alkylation with phenol [39], enzymes catalyzed aldol reaction [34,40] or polymerization with furan [41].

Nevertheless, in all these works, carbon balances were very low or even not reported, underlining the lack of products characterization and the need to strengthen our efforts on this critical point. A better understanding of carbohydrate macromolecules

production would be a key factor to ensure an industrial development of pyrolysis oil hydroconversion. In this study, the macromolecules formation during the catalytic hydroconversion of D-glucose and furfural, chosen to mimic compounds resulting from degradation of cellulose and hemicelluloses respectively, was investigated. The effect of reaction time and temperature as well as the presence of free water on macromolecules formation have been investigated.

2. Materials and methods

2.1. Material

The D-glucose (purity >99.5%) and furfural (purity 99%) were purchased from Sigma Aldrich (USA) and were used without any further treatment. N-hexadecane (purity 99%) was obtained from Alfa Aesar (USA) and will be referred as n-C16. Tetrahydrofuran (purity 99.7% min) was obtained from VWR.

A commercial NiMo/ γ -Al₂O₃ catalyst was supplied by Axens. Prior to catalytic test, the fresh catalyst was crushed and sieved to a particle size from 1 to 2 mm and subsequently reduced at 400 °C under H₂ flow (0.030 m³ h⁻¹) at atmospheric temperature and pressure for 2 h.

2.2. Experimental procedures

All catalytic tests were carried out in an isothermal 500 cm³ stainless steel autoclave equipped with an electromagnetic driven stirrer (Rushton impeller). For each run, 150 g of feed were introduced followed by 15 g of freshly reduced catalyst transferred in a basket in an argon vessel avoiding any post-oxidation. The reactor was hermetically closed and purged by substituting air by N₂ and finally by H₂. The initial pressure of H₂ was set to 3.0 MPa before temperature increase. The reaction temperature varied from 200 to 300 °C. To investigate water effect and in order to limit the thermal degradation of reactants during the heating ramp (15 min to reach 250 °C), the feed was vigorously stirred (1200 tr min⁻¹) either from the beginning of the experiment or only once the reaction temperature was reached. For comparison, some experiments where the feed was stirred during the heating ramp are also reported. This optimization has been done considering the maximization of the H₂ consumption during the catalytic hydroconversion of an aqueous D-glucose (20 wt%) solution. Those stirring rates and catalyst granulometries were chosen in order to optimize H₂ consumption (see Supplementary Figs. S2 and S3).

The H₂ addition was set to maintain a constant total pressure of 13 MPa during the run. Once the reaction time was reached, H₂ introduction was stopped and the reactor was cooled down to room temperature (10 min to cool down from 300 to 100 °C). The separation procedure is fully described in Supplementary Fig. S1. Gases were collected using an auxiliary vessel and sampled in vacuum TEDLAR[®] bags for subsequent off-line gas chromatography (GC-FID/TCD) analysis. While the reactor was purged by N₂ and unlocked, the catalytic basket was removed. The liquid phases and the solid residues were separated by centrifugation at 4000 tr min⁻¹ during 20 min. Subsequently, aqueous and organic phases (when n-hexadecane was introduced) were separated in a separatory funnel referred respectively as “aqueous phase” and “organic phase”. The recovered catalyst was washed using a Thermo Scientific™ Dionex™ (ASE 150) extractor heated at 60 °C and under a 10 MPa acetone pressure. The catalyst and the solid residues were dried at 70 °C under atmospheric pressure during 12 h. Acetone was used as a washing solvent also to clean the reactor and the impeller and was further removed by a vacuum rotary evaporator. The obtained liquid phase will be referred as

“washed phase”. The products were stored at $-20\text{ }^{\circ}\text{C}$ in order to limit the aging effects [42].

2.3. Analytical procedures

Considering the complexity of the products, an analytical strategy was set to characterize each effluent.

Gases were analyzed by a gas phase chromatograph Agilent 7890A equipped with a Flame Ionization Detector (FID) and two Thermal Conductivity Detectors (TCD). Three parallel columns were used: HP-Plot Q ($30\text{ m} \times 0.32\text{ mm i.d.} \times 20\text{ }\mu\text{m}$), HP-Plot 5A ($30\text{ m} \times 0.32\text{ mm i.d.} \times 1\text{ }\mu\text{m}$) and PONA ($50\text{ m} \times 0.2\text{ mm i.d.} \times 0.5\text{ }\mu\text{m}$). The carrier gas was helium. Standards were periodically injected for alkanes ($\text{C}_1\text{--}\text{C}_6$), CO, CO_2 , N_2 and H_2 quantification. The oven temperature program ranged from 30 to $200\text{ }^{\circ}\text{C}$ at a rate of $20\text{ }^{\circ}\text{C min}^{-1}$. The calculated H_2 consumption was the difference between introduced H_2 and GC-assessed H_2 contained in the swab tank. The mass of each quantified compounds was calculated with the ideal gas law knowing the pressure, the ambient temperature and the volume (0.015 m^3) of the swab tank.

D-glucose liquid effluents were analyzed on an Agilent 6890N gas chromatograph equipped with a FID and a split/splitless injector. Separation was performed with a mid-polar Rtx-35 Amine column (Restek, $30\text{ m} \times 0.25\text{ mm i.d.} \times 1\text{ }\mu\text{m}$) with a $53.3\text{ cm}^3\text{ min}^{-1}$ constant helium carrier gas flow rate. Inlet was set to $250\text{ }^{\circ}\text{C}$ with a split ratio of 35, while the oven temperature program ranged from 40 to $220\text{ }^{\circ}\text{C}$ at a rate of $4\text{ }^{\circ}\text{C min}^{-1}$. This column was adopted after comparison of the peaks resolution with the less-polar PONA column used for furfural. Furfural liquid effluents were analyzed by GC (AGILENT-6890N) equipped with PONA column (Agilent J&W, $50\text{ m} \times 0.20\text{ mm i.d.} \times 0.5\text{ }\mu\text{m}$). A $35.8\text{ cm}^3\text{ min}^{-1}$ constant helium carrier gas flow rate was set. Inlet was set to $280\text{ }^{\circ}\text{C}$ with a split ratio of 50, the oven temperature program ranged from 100 to $250\text{ }^{\circ}\text{C}$ at a rate of $5\text{ }^{\circ}\text{C min}^{-1}$. For each identified compounds, quantification was performed with propane-1,2-diol as an external standard and Effective Carbon Number method (ECN) was used to estimate FID response factors for oxygenates [43]. GC/MS experiments that led to the identification of compounds were conducted on a Thermo Trace GC-MS using the same analytical conditions than those used for the GC-FID analysis. The mass analyzer was a single quadrupole ($m/z = 10\text{--}500$) and electron impact ion source was used in a positive mode (EI+, 70 eV). Products were identified using the NIST library (2009). During the identification process, in the worst cases, the accepted probability percentage was at least above 80%.

The composition of the liquid phase from the D-glucose conversions was also determined using a high performance liquid chromatography HPLC system (Waters Alliance 2695), a Bio-Rad Aminex Deashing column followed by an Agilent Metacarb column operated at $95\text{ }^{\circ}\text{C}$. The aqueous mobile phase was set at a flow rate of $0.4\text{ cm}^3\text{ min}^{-1}$. Detections were performed by a Differential Index Refractometer (RID) and a UV analytical system. The analysis for one sample was completed within 120 min. The concentration of the carbohydrate compounds (cellobiose, D-glucose, sorbitol, xylose, galactose, arabinose, mannose, glycerol and xylitol) in the product mixture was determined using RID calibration curves obtained from standard solutions (see Supplementary Fig. S4).

To get an insight of D-glucose conversion products, one liquid effluent was also analyzed by a preparative HPLC-UV (ATLANTIS-T3) on a reversed phase column operated at $35\text{ }^{\circ}\text{C}$. The aqueous-methanol mobile phase was set at a flow rate of $1.3\text{ cm}^3\text{ min}^{-1}$. The analysis for a sample was done in 30 min. Recovered fractions were subsequently analyzed by a Fourier Transform Ion Cyclotron Resonance Mass Spectrometry (FT-ICR/MS). The Thermo LTQ Ultra mass spectrometer is a hybrid mass spectrometer coupling a linear ion trap (LTQ) and an FT-ICR mass analyzer. The magnet is an

Oxford with a 7 T magnetic field. The Electrospray Ionization (ESI) ion source was used in positive ion mode with a voltage of -4 kV in flow injection at $5.10^{-6}\text{ m}^3\text{ min}^{-1}$. This mode was initially adopted to specifically detect D-glucose and its oligomers. The tune of the mass spectrometer was done with the tune mix ESI of Thermo Scientific, the mass error was less than 1 ppm and the mass spectral resolution was 100 k at 350 m/z . In-house developed software [44] was used to calculate the components raw formulas assuming the presence of atoms of carbon (from 0 to 50), hydrogen (from 0 to 100), oxygen (from 0 to 15) and sodium (from 0 to 1 as adduct) as well as taking into account a CH_2O Kendrick mass defect.

Water content in liquid effluents was measured by a Karl Fischer Mettler Toledo V.20 (reported data are expressed as an average of three measurements). Before each analytical sequence, a calibration procedure involved a Fluka Hydranal 1.0 standard.

Soluble macromolecules contained in aqueous effluents were analyzed by size exclusion chromatography (SEC) with a Waters system (Alliance). The system was constituted by four columns in series ($7.8 \times 300\text{ mm}$, particle size $5\text{ }\mu\text{m}$). During a typical analysis 50.10^{-6} m^3 of sample were injected into the column. Run were performed at $30\text{ }^{\circ}\text{C}$ (columns temperature) during 49 min. Two detectors were used: a refractive index-detector and a UV-detector set to 254 nm chosen for its specific detection of carbonyls and aromatic of selected model molecules (furfural, acetaldehyde, 1,2-benzenediol, guaiacol, 5-HMF, xyleneol and benzofuran). Tetrahydrofuran was used as mobile phase ($1\text{ cm}^3\text{ min}^{-1}$). Seven standard polystyrene (noted as PS) having various molecular weights were analyzed at the beginning of each new sequence. This calibration procedure allows molecular weight detection ranging from 160 to 5000 g mol^{-1} (see Supplementary Fig. S4).

In order to ascertain the carbon balance, a Thermo Scientific™ FLASH 2000 was used to measure the amount of carbon deposit that was present on the catalyst and on the solid residues. Grinded samples were injected twice in an oven set at $950\text{ }^{\circ}\text{C}$ where CO_2 was formed. An on-line TCD detector quantified this component and calculated the sample corresponding carbon equivalent. Each six samples, the analyzer was controlled by a BBOT (2,5-bis (5-*tert*-butyl-benzoxazol-2-yl)thiophene) standard.

Solid phase ^{13}C MAS NMR experiments were performed on an AVANCE Bruker 400 MHz spectrometer with Highpower Proton Decoupling (HPDEC) and spinning rates of 12 kHz using a CPMAS probe and a 4 mm rotor. The free induction decays were obtained after excitation with 90° pulses with a repetition time of 50 s. After accumulation of 1024 scans, spectra were processed with 20 Hz Lorentzian line broadening and a 0.1 s Gaussian broadening. All ^{13}C MAS NMR spectra were referenced to tetramethyl silane (TMS). Quantitation of the functional groups present in each sample was determined after baseline correction by integrating over characteristic regions using TopSpin 3.0 software. Intensities over defined chemical shift windows were integrated to quantify selected C structures; 0–55 ppm (C-alkyl), 55–95 ppm (O-alkyl C including carbohydrates), 95–165 ppm (C-aromatic), 165–220 ppm (C-carbonyl in carboxylic acids, esters, amides, ketones and aldehydes).

2.4. Determination of conversion, selectivity and carbon balance

This study aims at understanding D-glucose and furfural hydroconversion from the macroscopic scale (though experimental balance given by Equation (1)) to the molecular scale. In order to assess the accuracy of chemical pathways, carbon balances were considered taking into account each recovered phase as detailed in Equation (2). Total Organic Carbon (TOC) in the liquid products has not been considered because of the presence of n-hexadecane.

Mass balance

Experimental mass loss (expressed in weight %)

$$= \frac{\left(m_{\text{liquid}} + m_{\text{gases}} + m_{\text{catalyst}}\right)_{\text{introduced}} - \left(m_{\text{liquid}} + m_{\text{gases}} + m_{\text{catalyst}} + m_{\text{residues}}\right)_{\text{recovered}}}{\left(m_{\text{liquid}} + m_{\text{gases}} + m_{\text{catalyst}}\right)_{\text{introduced}}} \times 100 \quad (1)$$

Carbon balance

Total quantified carbon (expressed in weight % of carbon equivalent)

$$= \frac{\left(mC_{\text{liquid}}\right)_{\text{introduced}} - \left(mC_{\text{liquid}} + mC_{\text{gases}} + mC_{\text{catalyst}} + mC_{\text{residues}}\right)_{\text{recovered}}}{\left(mC_{\text{liquid}}\right)_{\text{introduced}}} \times 100 \quad (2)$$

Recovered carbon amount corresponds to equivalent carbon quantified from GC-FID and HPLC analysis of liquid products, GC-FID/TCD analyses of the gaseous products and elementary analyses (CHNS) of the solid residues and the catalyst. Solving the Equation (2) implies considering the carbon contribution of each quantified species.

Hence, carbon contribution of a molecule so called “j” and “k” constituted of carbon, oxygen and hydrogen atoms leads to the following equation:

$$mC_j = \text{wt}\%C_j \cdot m_j \quad \text{and} \quad mC_{\text{liquid}} = \sum_{i=j}^k mCi \quad (3)$$

With:

- mC_j : mass of carbon equivalent in the compound j [g].
- $\text{wt}\%C_j$: weight carbon content of the compound j [wt%].
- m_j : mass of quantified compound j [g].
- $\sum_{i=j}^k mCi$: sum of the carbon equivalents holds by the compounds “j” to “k” in the liquid phase [g].

To consider the molecular scale, reactant (expressed as “A”) conversion and products (expressed as “j” and “k”) selectivity will be expressed as:

$$X_i = \frac{n_{A,0} - n_A}{n_{A,0}} \quad S_j = \frac{n_j}{\sum_{i=j}^k ni} \quad (4)$$

With:

- X_A : conversion rate of “A” reactant
- S_j : product “j” selectivity [mol mol⁻¹].
- $n_{A,0}$ and n_A : “A” reactant molar amount respectively at the beginning and the end of the reaction [mol].
- n_j : “j” product molar amount at the end of the reaction [mol].
- $\sum_{i=j}^k ni$: sum of the molar amounts of the compounds “j” to “k” in the liquid phase [g].

Molecular weight distributions of liquid products were corrected using Equation (5) to take into account the water content of each sample that was analyzed by size exclusion chromatography.

$$\begin{aligned} \text{Normalized SEC signal} &= \frac{\text{Raw signal}}{100 \text{ mg}} \cdot \frac{1}{1 - \text{Water content}} \\ &= \frac{\text{Raw signal}}{100 \text{ mg}} \cdot \frac{1}{\text{Organic content}} \end{aligned} \quad (5)$$

With:

- Raw signal.100 mg⁻¹: $m_{\text{liquid fraction}}$: Raw signal (RI or UV) normalized to a 100 mg sample [mg⁻¹].
- Water content: weight water content in the liquid phase [-].
- Organic content: weight organic content in the liquid phase [-].

The water balance determined for the liquid phases is expressed as:

$$\frac{\text{Recovered water}}{\text{Introduced water}} = \frac{m_{\text{liquid fraction}} \cdot \text{Water content}}{m_{\text{Introduced water}}} \quad (6)$$

With:

- $m_{\text{liquid fraction}}$: mass of recovered liquid fraction weight [g].
- Water content: weight water content in the liquid phase titrated by Karl Fisher analysis [wt%].
- $m_{\text{Introduced water}}$: mass of water initially introduced in the model compounds mixture [g].

The carbon content of solids resulting from D-glucose hydro-conversion during a test “i” containing n-hexadecane (noted as n-C16) onto the surface assessed by solid ¹³C MAS NMR. Hexadecane was calibrated thanks to an external calibration (see supplementary Fig. S4). Due to the intensity of hexadecane chemical shifts, the corresponding areas were calculated and further subtracted to the ¹³C NMR spectra. Thus, carbon equivalent in the solid residues were calculated following Equation (7).

$$m_{\text{cor } i} = m_{\text{raw } i} - m_{\text{n-C16}} \quad (7)$$

With:

- $m_{\text{cor } i}$: corrected mass of carbon equivalent in the residues for a test “i” [g].
- $m_{\text{raw } i}$: mass of carbon equivalent in the residues measured by elementary analysis for a test “i” [g].

- m_{n-C16} : mass of Carbon equivalent brought by n-hexadecane in the solid residues quantified by ^{13}C MAS NMR external calibration [g].

3. Results and discussion

3.1. Furfural catalytic hydroconversion

3.1.1. Effect of temperature and reaction time

The catalytic hydroconversion of furfural (13 wt%) in water (30 wt%) and n-hexadecane (57 wt%) will be discussed herein. Feed was maintained under stirring during the heating time period. N-hexadecane was used as a non-reactive compound to fill the reactor up to 150 g.

The experimental mass balances presented in Table 1 evidence a correct recovery procedure of the products allowing us to consider the carbon balance in all fractions. Various effects can be observed depending on time and temperature. At 250 °C, furfural conversion raised from 53 to 100% during the first hour of reaction, as well as for all other experiments. In addition, at a fixed reaction time of one hour, H_2 consumption increased by 35% between 200 and 300 °C evidencing an enhancement of hydrogenation and hydrogenolysis reactions by increasing the temperature. However, the temperature did not impact drastically the mass of recovered phases and no significant solid residues were observed apart from the carbon deposit onto the catalyst.

The HDC of furfural is extensively reported in the literature [35,38] and our reaction network built from 35 GC-analyzed compounds in the liquid phases confirms the main pathways (Supplementary Fig. S5, S6 and Table S1).

To assess the GC quantifications, it appeared mandatory to take into account carbon balances. The furfural introduction in the feed represents initially 12.5 g of carbon equivalent while no significant carbon deposition was measured by elementary analysis of the fresh reduced catalyst. The heaviest quantified compounds by GC-

FID were valeric acid, 2-tetrahydrofurylmethylether and tetrahydro((tetrahydrofuryl)methoxy)-2H-pyran. Table 2 summarizes the equivalent carbon balances corresponding to compounds quantified. Balances also take into account the carbon deposited on the catalyst (ranging from 4 to 6 wt% of the recovered catalysts) and constituting the solid residues. The general trend shows an increase of temperature and/or residence time responsible for a loss of quantified carbonaceous species in the liquid phase. Between t_0 and after 3 h of reaction, the total carbon balance dropped from 72.4 to 32.9% at 250 °C.

The molecular weights measured by SEC-RI analyses are reported in Fig. 1 and evidence the formation of heavy compounds up to 500 g mol⁻¹ PS eq. (referring to polystyrene equivalent). This is concomitant with the assumptions related to the loss of the carbon in the liquid phase as reported in Table 2. Indeed, at a constant reaction time, amount of the heavy molecular weight compounds increases as a function of the temperature. Such compounds, not quantified by GC-FID, contribute to the loss of the carbon balances. The important variations observed may indicate that the nature of the products and the reaction pathway vary as a function of the reaction temperature.

To conclude, it appears to be mandatory to take into account the formation of soluble macromolecules. This original approach that considers both carbon balances and SEC analysis is required for the understanding of water impact studied hereafter.

3.1.2. Effect of water

In order to limit furfural thermal degradation, effect of water was investigated without stirring during the heating ramp. In those experiments, water content varied from 0 to 87 wt% while furfural concentration was kept constant (i.e. 13 wt% of the initial model compounds mixture). In order to complete the feed, n-hexadecane was introduced, representing from 0 to 87 wt% of the initial feed.

To better understand the catalyst behavior in presence of water, a test had also been performed with a water content of 1.3 wt%. This

Table 1
Furfural catalytic hydroconversion experimental balances.

T (°C)		200		250			300	
t (h)		1	3	0	1	3	1	3
Inlet	Liquid phase (g)	150.0						
	Reduced catalyst (g)	14.2	14.2	14.4	14.2	14.1	14.2	14.2
	Introduced H_2 (g)	4.5	4.6	1.0	3.6	3.7	2.0	2.2
Outlet	Liquid phase (g)	149.6	148.4	148.5	145.2	143.5	141.0	147.0
	Gaseous phase without H_2 (g)	2.8	2.8	1.2	2.6	2.6	3.1	2.6
	Solids (g)	0.0	0.2	0.2	0.3	0.0	0.1	0.4
	Catalyst (g)	16.6	15.1	15.7	15.8	16.1	15.6	15.5
	Loss (wt%)	-0.2	1.3	-0.2	2.4	3.4	3.8	0.5
	H_2 consumption/introduced	0.3	0.4	0.3	0.4	0.4	0.5	0.6
	Furfural conversion (%)	100.0	100.0	53.0	100.0	100.0	100.0	100.0

Table 2
Furfural catalytic hydroconversion carbon balances.

T (°C)		200		250			300	
t (h)		1	3	0	1	3	1	3
Liquid phase by GC/FID		3.0	5.8	7.6	4.1	2.9	3.4	2.0
g of C								
Catalyst and solids residues by elementary analysis		0.9	0.8	0.8	0.9	0.9	0.8	0.8
g of C								
Gas phase by GC/FID-TCD		0.1	0.1	0.2	0.3	0.2	0.8	0.6
g of C								
Total detected carbon		4.0 (32.9)	6.7 (56.0)	8.7 (72.4)	6.2 (49.7)	3.9 (32.9)	5.1 (42.3)	3.5 (29.1)
g of C (wt%)								

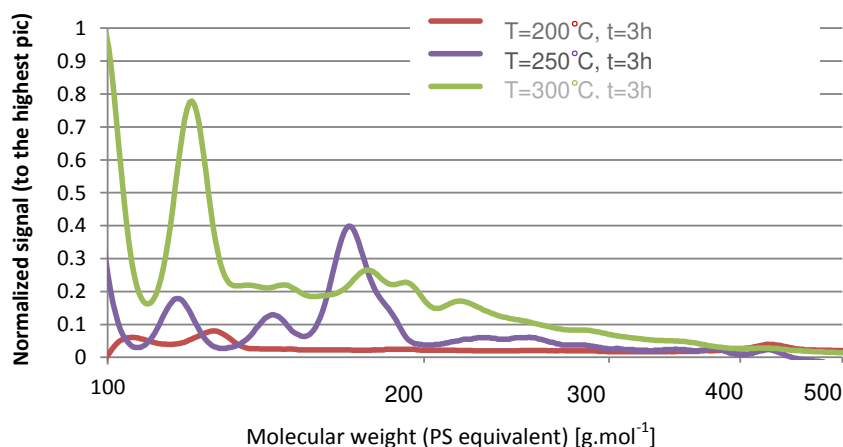


Fig. 1. SEC-RI chromatogram of furfural catalytic hydroconversion liquid effluents.

amount represents the theoretical limit of wettability of the catalyst when the whole porosity was covered by water. This calculation takes into account the theoretical alumina surface impregnation proposed by Nédez [45] with a margin of error of 20%.

The temperature and the reaction time were set respectively at 250 °C and 1 h. Experimental mass balances are reported in Supplementary (Table S2). Furfural HDC does not produce solid residues for all operating conditions. Moreover, no drastic variations were observed concerning the other recovered fractions.

To go further in the description, the corresponding molecular analysis were reported in Supplementary data (Supplementary Figs. S7 and S8). To assess the molecular description of the system, carbon balances are reported in Table 3. It is important to note the drastic decrease of the quantified products in the liquid phases when water was introduced to the medium up to 8 wt%.

Table 3 shows that the most dramatic variation of carbon balance was related to carbonaceous compounds present in the liquid fractions. A loss of carbon was observed while water content progressively increased in the medium. On the other hand, the test carried out with 87 wt% of n-hexadecane (no introduced water) showed a good closure of the carbon balance (82.6%). When water content was higher, the quantification in the liquid phase dropped, which suggests that heavy soluble molecules were formed but not quantified by GC-FID.

To get an insight of soluble macromolecules contained in aqueous phases, molecular weight distributions measured by SEC-RI are reported in Fig. 2. SEC data were normalized to take into account the introduced mass sample and also the mass of water (Equation (5)) preventing any artificial dilution of macromolecules by the amount of water. Water contents titrated by the Karl Fisher method are presented in Supplementary data (Supplementary

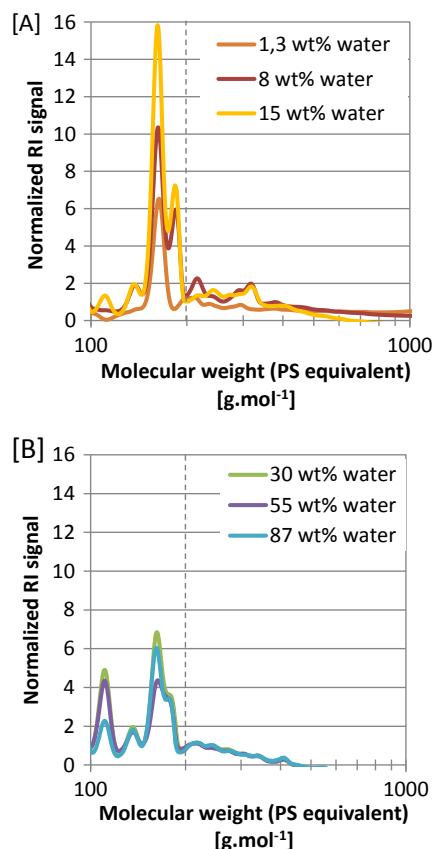


Fig. 2. SEC-RI chromatograms of furfural effluents at various initial water introductions [A] from 1.3 to 15 wt%, [B] from 30 to 87 wt%.

Table 3
Water effect on furfural catalytic hydroconversion carbon balances.

Initial water content (wt%)	0	1.3	8	15	30	55	87
Liquid phase by GC/FID g of C	8.4	7.5	5.2	5.0	4.8	4.2	4.9
Catalyst and solids residues by elementary analysis g of C	1.2	0.9	0.9	0.5	0.7	0.6	0.4
Gas phase by GC/FID-TCD g of C	0.4	0.2	0.1	0.2	0.2	0.2	0.5
Total detected carbon g of C (wt%)	10 (82.6)	8.7 (64.6)	5.3 (44.0)	5.6 (46.9)	5.7 (47.7)	5.0 (41.6)	5.8 (48.1)

Table S2).

Fig. 2[A] reports SEC-RI detection profiles for the fractions obtained with an initial water content between 1.3 and 15 wt%. Although this analysis is not quantitative, regarding the similarities of the profiles, we assumed that a direct comparison of the normalized intensities can be done. Then, the amount of soluble macromolecules raised a maximum of intensity for 15 wt% water content. At this latter water content, the GC-quantified carbon in the liquid (Table 3) remained low. Up to this loading, water effect remained detrimental with a similar macromolecules formation.

It can be emphasized that the variations observed between 100 and 200 g mol⁻¹ corresponds to the predominance of a specific reaction pathway. However, this trend was not further observed above 30 wt% of water as presented in Fig. 2[B]. At such high water content, the amount of soluble macromolecules (molecular weight higher than 200 g mol⁻¹ eq. PS) did not further increase as it is also shown by the stabilization of carbon balances (Table 3).

3.2. D-glucose catalytic hydroconversion

3.2.1. Effect of temperature and reaction time

The D-glucose HDC experiments (20 wt%) in water medium (80 wt%) were carried out with stirring during the heating time period. All the tests were performed in batch conditions with 150 g of feed and 15 g of reduced catalyst. In those experiments, the

conversion of D-glucose reached 100%, except when the reaction was stopped right after reaching 200 °C (study of the heating period).

The experimental mass balances are presented in Supplementary (Supplementary Table S3). Mass losses were below 10 wt% and enabled to consider the carbon balance represented through all phases. The increase of temperature and residence time involves a rise of the gaseous formation and the solid residues deposition onto the catalyst. Nevertheless, the experimental mass balances did not evolve between 1 and 3 h of reaction, showing the importance of the first minutes (including the heating period) of reaction. Indeed, during the heating period at 200 °C, D-glucose was converted up to 82%.

The chromatographic analysis of liquid phase enables the identification and quantification of 46 organic compounds (Supplementary Table S4). The extended reaction pathway reported in Fig. 3 is only based on HPLC and GC identified products containing between one and six carbon atoms. Under our operating conditions, many different reactions occurred including C-C hydrogenolysis (production of levulinic acid or furfural), hydrogenation (production of sorbitol [30] and alcohol compounds from ketones), dehydration/hydration (production of 5-HMF or lactic acid) retro-aldol reaction (production of propane-1,2,3-triol and propane-1,2-diol [26]), decarboxylation or decarbonylation. Carboxylic acids (acetic acid, levulinic acid) were widely produced and

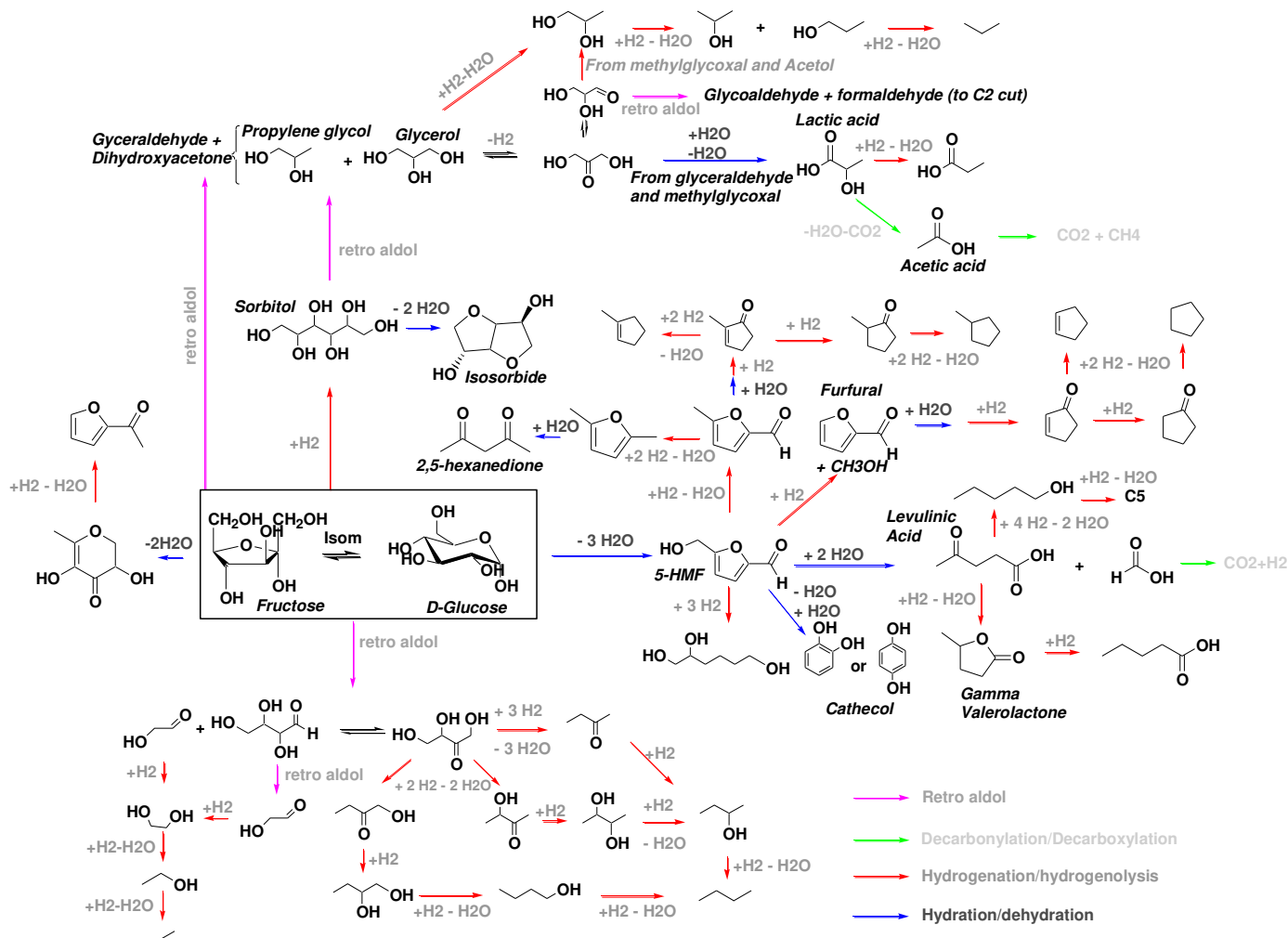


Fig. 3. : D-glucose catalytic hydroconversion pathways from GC-FID and HPLC-RI analysis.

Table 4

D-glucose catalytic hydroconversion carbon balances.

T (°C)	200			250		300	
t (h)	0	1	3	1	3	0	3
Liquid phase by GC/FID g of C	4.9	4.1	5.0	1.9	2.2	1.5	1.8
Catalyst and solids residues by elementary analysis g of C	0.5	0.6	0.6	1.4	2.1	1.1	0.8
Gas phase by GC/FID-TCD g of C	0.3	0.3	0.5	0.7	0.7	1.9	2.2
Total detected carbon g of C (wt%)	5.7 (47.3)	5.0 (41.9)	6.1 (51.2)	4.0 (33.3)	4.9 (41.1)	4.5 (37.7)	4.9 (40.5)

contribute to a low pH ranging from 2 to 3. Few fully deoxygenated light compounds were observed in the gaseous phase.

The carbon balances based on those quantified compounds are reported in Table 4.

The initial feed of D-glucose represents 12 g of carbon equivalent. In the liquid phase, sorbitol was the heaviest component ($M_w = 181 \text{ g mol}^{-1}$) that was quantified by HPLC-RI. Liquid products that have a higher molecular weight were considered as soluble macromolecules. Most of the lighter compounds were quantified either by GC-FID or by HPLC-RI. Some components such as propane-1,2,3-triol or 5-(hydroxymethyl)-2-furaldehyde were both quantified by GC-FID and HPLC-RI in similar concentrations (uncertainty of less than 10%).

Literature studies usually do not include carbon mass balance in addition of the molecular description. In this study, the carbon balance taken into account includes total carbon content, from gaseous to liquid phases and also the carbon deposited onto the catalyst (ranging from 4 to 6 wt% of the recovered catalysts) and the solid residues (ranging from 60 to 70 wt% of the recovered residues). Then, it is interesting to note the drop of quantified compounds in the liquid phase on the contrary to the gaseous phase, when the temperature increased. Despite of that, the total quantified carbon decreased with the temperature. All in all, total identified carbon was never beyond 51.2% of the initial introduced carbon equivalent. The low carbon balance observed for all the experiments is likely due to the presence of a large amount of heavy molecular weight products in the liquid phase.

To go further on those three liquid effluents, SEC-RI analyses are reported in Fig. 4[A]. It can be observed soluble macromolecules with molecular weight higher than 700 g mol^{-1} PS eq. (referring to polystyrene equivalent). For catalytic hydroconversion experiments performed at 200°C , reaction time does not seem to influence the molecular weight distribution of the liquid phases. When the HDC temperature was increased to 250°C , intensity of normalized SEC-RI chromatograms decreased while the amount of carbon deposit onto the catalyst increased. This may indicate that soluble macromolecules were mainly produced at higher temperature and further precipitated onto the catalyst. As indicated by Fig. 4[A], those solid precursors were water-soluble until 700 g mol^{-1} PS eq. Those results are in accordance with the low carbon balances previously described.

Regarding the low carbon balances and SEC analyses it would be irrelevant to describe the products selectivity of the entire chemical network. Nevertheless, quantified compounds (by GC-FID/TCD and HPLC-RI) can be sorted by cuts (number of carbons) from both gaseous and liquid phases. The Fig. 4[B] shows the molecular products distribution at two temperatures. Because of the important variation of quantified compounds, it is more pertinent to sort them by reaction temperature. As previously observed, most of the reactions occurs before 1 h of hydroconversion. Then a 50°C increase of the temperature reaction leads to a dramatic decrease of

the quantified compounds due to the heavy compounds formation. CH_4 and CO_2 analyses demonstrate that equilibriums described by Equations 8 and 9 (reported in Supplementary) were not prevailing in those conditions. Indeed, CO and CH_4 quantifications did not vary but CO_2 amount increases between 200 and 250°C probably through decarboxylation reactions.

Despite of the lack of molecular data provided by GC and HPLC analyses, the complementary description of our system through the carbon balance and the SEC analysis allowed to improve the understanding of the D-glucose reaction scheme. It appears to be essential to cross those analyses in order to investigate the impact

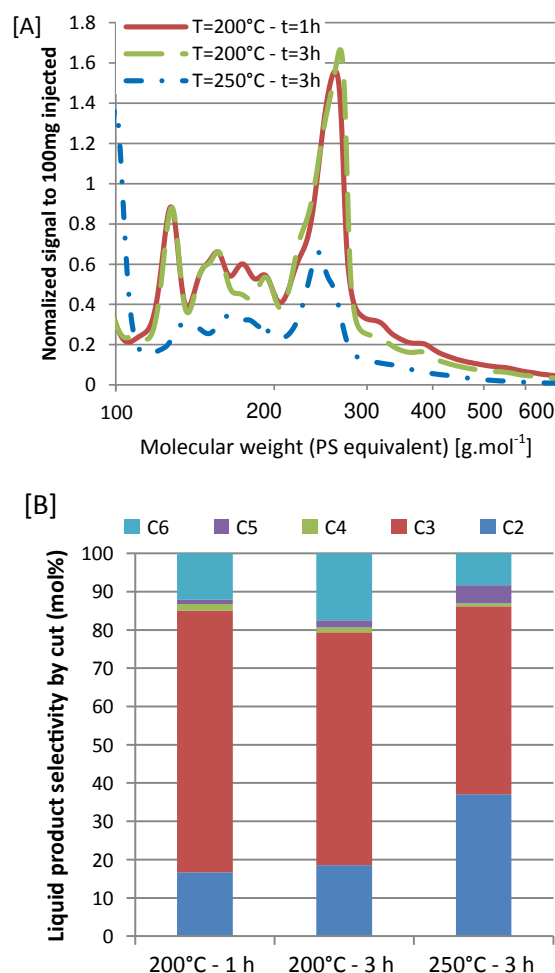


Fig. 4. : D-glucose catalytic hydroconversion [A] SEC-RI analyses of liquid effluents [B] Selectivity of quantified products in liquid phase by GC and HPLC gathered by cuts.

of water on the D-glucose HDC.

3.2.2. Effect of water

In order to limit D-glucose thermal degradations, effect of water has been assessed without stirring during the heating ramp. D-glucose initial content was maintained to 20 wt%. In order to investigate the effect of water, the initial amount of water in the feed has been varied from 80 to 30 wt%. To insure D-glucose solubility at room temperature, at least 20 wt% of water is needed in the feed. In order to complete the feed to 100%, n-hexadecane has been introduced respectively from 0 to 50 wt%. The temperature and the time of reaction were set respectively to 250 °C and 1 h.

The experimental mass balances, H₂ consumption rate and the D-glucose conversion obtained for these experiments are reported in Table 5. The conversion of D-glucose reached 100% for all experimental conditions. The solid formation clearly decreased from 11.9 to 2.4 g when water content increased respectively from 30 to 80 wt%. Carbon balances (Equation (2)) are reported in Table 6. The amount of carbon released in the gaseous phase was relatively stable independently of the water content of the feed and quantified species were mostly CH₄, CO and CO₂. Recovered solid residues represent the main source of carbon equivalent ranging from 26.6 to 60.0 wt% of the initial introduced carbon (12 g coming from D-glucose).

To get a better insight on the composition of solid residues, ¹³C MAS NMR spectra have been recorded on the acetone washed and dried samples in direct polarization in order to be quantitative. The ¹³C spectra obtained for the four residues were comparable to the one illustrated in Supplementary data (Supplementary Fig. S9) that may indicate the presence of residues with such similar C-structures obtained after similar reaction route. Solids residues were mostly composed by aromatic (50–60 atomic %C) and aliphatic (25–30 atomic %C) functional groups. This suggests that soluble macromolecules from which arise solid residues were also composed by aromatics. ¹³C MAS NMR spectra of residues obtained with 30–60 wt% water revealed four additional well defined compounds in the aliphatic region ($\delta_{\text{TMS}} = 32, 30, 22$ and 14 ppm) that were relative to n-hexadecane. The intensity of these

contributions increased as a function of the initial concentration of hexadecane introduced. The presence of hexadecane in the residues recovered after test was not expected and could be due to a deposition onto the solid porosity. Thanks to an external calibration, the amount of hexadecane has been assessed (Equation (7)) and taken into account in carbon balances (Table 6).

The carbon balances reported in Table 6 also indicate that the equivalent amount of carbon provided by the characterized compounds by GC and HPLC analyses in the liquid fractions decreased. As water was introduced from 30 to 80 wt%, quantified carbon represented respectively only 5.9 to 10 wt% of the initial introduced carbon. Considering the total organic carbon (TOC) measurement of the 80 wt% water experiment, 6.8 g of carbon was titrated that indicates a molecular quantification of only 17.6 wt% of recovered carbon in the liquid phase.

The quantified products which, possess 1 to 6 carbon atoms are reported in Supplementary data (Supplementary Fig. S10). However, the analysis performed by GC-FID and HPLC were not prone to detect more than 10 wt% of the initial introduced carbon (Table 6). To get an insight of the liquid composition, normalized (Equation (5)) SEC analyses are reported in Fig. 5.

According to Fig. 5[A], an important variation of the molecular weight distribution intensity measured by SEC-RI from aqueous fractions can be seen. Even, if this analysis is not quantitative, regarding the similarities of the profiles, we assumed that a direct comparison of the normalized intensities can be done. Thus, a higher amount of soluble macromolecules was quantified when water was introduced in large quantities. The Fig. 5[B] represents molecular weight distributions measured by SEC-UV at 254 nm. This wavelength was preferably used to detect aromatics and carbonyls species and demonstrates the occurrence of such molecules up to 1000 g mol⁻¹ PS eq.

When water was introduced from 45 to 80 wt%, SEC analyses reported in the Fig. 5[A] and [B] show an increase of the proportion of soluble macromolecules. Below 45 wt% water, the solid formation grows to a maximum but analyses show a subsequent increase of macromolecules amount indicating a high macromolecules formation in parallel to the solid formation. Contrary to furfural, the

Table 5
Water effect on D-glucose catalytic hydroconversion experimental balances.

	Initial water content (wt%)	30	37.5	45	60	80
Inlet	Liquid phase (g)	150.0	150.0	150.0	150.0	150.0
	Reduced catalyst (g)	14.3	14.4	14.3	14.3	14.3
	Introduced H ₂ (g)	2.7	2.6	2.4	2.7	2.5
Outlet	Liquid phase (g)	105.6	124.7	138.8	136.8	143.1
	Gaseous phase without H ₂ (g)	2.5	2.4	2.7	2.6	2.4
	Solids (g)	11.9	9.5	6.2	6.5	2.4
	Catalyst (g)	18.5	17.0	17.4	17.4	16.7
	Loss (wt%)	15.5	6.7	1.0	2.2	1.3
	H ₂ consumption/introduced	0.2	0.2	0.1	0.2	0.2
	D-glucose conversion (%)	100.0	100.0	100.0	100.0	100.0
	Water content in the aqueous phase (wt%)	86.9	88.5	74.9	87.4	93.6

Table 6
Water effect on D-glucose catalytic hydroconversion carbon balances.

Initial water content (wt%)	30	37.5	45	60	80
Liquid phase by GC/FID g of C	0.7	0.9	1.1	1.0	1.2
Catalyst and solids residues by elementary analysis g of C	7.2	7.9	5.8	5.9	3.2
Gas phase by GC/FID-TCD g of C	0.8	0.7	0.8	0.8	0.7
Total detected carbon g of C (wt%)	8.7 (72.3)	9.5 (79.0)	7.7 (64.0)	7.7 (64.0)	5.1 (42.6)

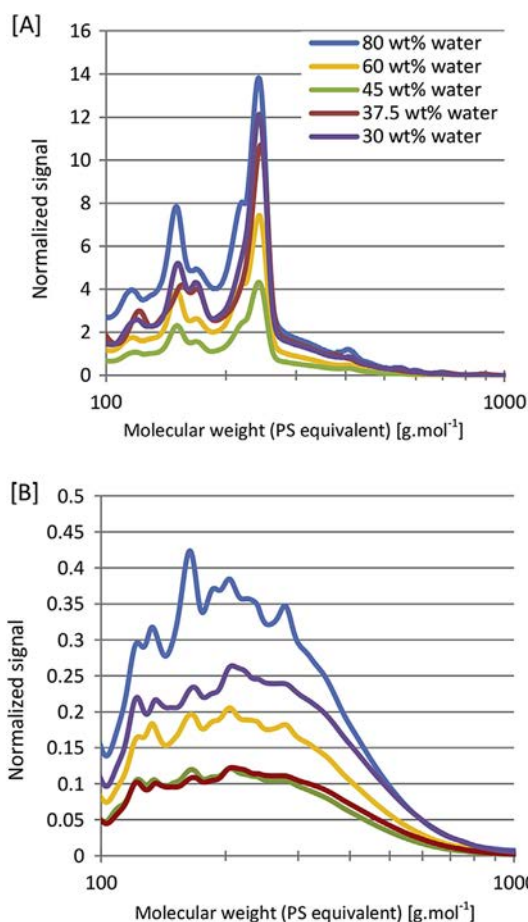


Fig. 5. SEC chromatograms of soluble macromolecules from D-glucose catalytic hydroconversion: [A] SEC-RI detection, [B] SEC-UV254 nm detection.

liquid phases molecular analyses did not indicate any modification pathway that can explain this variation. As previously shown by solid state ^{13}C NMR analyses, Fig. 5[B] indicates the presence of heavy molecular weight aromatic species. Then, it appears important to consider a physical effect through the solubilization equilibrium but also a chemical effect through the water consumption. Both effects are discussed hereafter.

3.3. Identification of macromolecules precursors and formation pathways

Both furfural and D-glucose hydroconversion led to the formation of high molecular weight macromolecules difficult to characterize. Our model compounds produced macromolecules soluble in the aqueous phase (up to 700 g mol^{-1} PS eq.) as it was observed in Figs. 4 and 5 in agreement with results from the literature [27,31,32].

In order to get a better insight of these macromolecules, the liquid effluent resulting from catalytic HDC of D-glucose in 80 wt% water at $200\text{ }^\circ\text{C}$ during one hour was physically fractionated using a preparative HPLC technique. This work aims at splitting a D-glucose effluent in several zones of elution by HPLC. Isolated and concentrated fractions (Supplementary Fig. S11) were firstly analyzed by a soft ionization and a simple quadrupole mass spectrometer. This step allows the detection of molecular ions for 9 fractions that were recovered and further analyzed using FT-ICR mass spectrometry (ESI + ionization).

In average 2100 peaks per fractions were observed between 50 and 500 m/z with an accuracy of 10^{-4} m/z . From those nine gathered fractions, 591 chemical formulas involving up to 26 atoms of carbon were calculated (see the complete list in Supplementary Table S5). The molecular mass distribution of those compounds and related O/C and H/C atomic ratios are reported in Fig. 6 [A] and [B]. Concomitantly with D-glucose carbon balance (Table 4) and SEC analysis (Fig. 4[A]), more than 70% of the detected overtook 200 g mol^{-1} (Fig. 6[A]). Moreover, those results are in line with the detection comparison of GC, GCxGC and FTICR-MS analysis applied to a bio-oil presented by our group [46]. Despite on this extensive detection, this Van Krevelen mapping could be improved by conducting a dedicated analytical study with an ESI- ionization.

According to these data, it is possible to propose some chemical structures. Thus, it was assumed that sugars oligomerization, ketones and hydrated furanic species can be precursors of higher molecular weight compounds via aldol condensation. Considering furanic species, they were prone to produce macromolecules by first hydration and then condensation. For instance, one relevant peak ($\text{C}_{12}\text{H}_{14}\text{O}_7$: $270.2358\text{ g mol}^{-1}$) corresponding to the red dot in

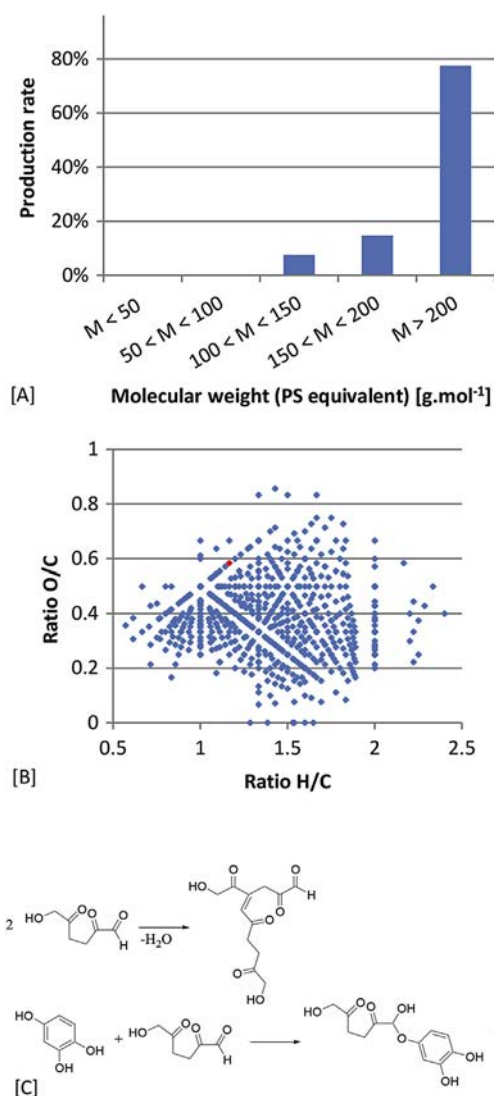


Fig. 6. FT-ICR/MS analysis of a D-glucose product conversion fraction; [A] Molecular weight distribution, [B] Van Krevelen diagram, [C] Proposed formation scheme for a $270.2358\text{ g mol}^{-1}$ compound.

Fig. 6[B] was analyzed. The pathways reported in Fig. 6[C] describes an aldol condensation of 2,5-dioxo-6-hydroxy-hexanal (as previously reported as DHH by Patil [31,32] and the hydration of 5-HMF to form benzenetriol further O-alkylated with a DHH molecule). Aromatics species were previously revealed by SEC (UV-254 nm detection) analysis in Fig. 5[B]. It can be also a precursor of solid residues characterized as aromatics by ^{13}C MAS NMR.

For both studied model molecules, it can be assumed that furanic compounds, such as 5-HMF, were key precursors for the formation of macromolecules. In any cases, water was involved as a reactant that impacts these undesired reactions depending on its introduced amount. In the case of D-glucose, the precursors were produced from non-catalytic pathways (tests without catalyst are reported in Supplementary Figs. S12 and S13) such as dehydration in homogeneous media producing furanic species followed by aldol condensation leading to high molecular weight compounds which readily precipitate. We can assume that their polarities and structures were no more compatible with the aqueous matrix in order to generate sufficient interactions for their solubilization. An interesting analogy can be proposed with the stabilization of asphaltenes by resins systems during the crude oil refining [47].

For Furfural, a different behavior was observed due to the ring opening occurring by hydrolysis reaction. This reaction route initiates the formation of macromolecules precursors such as 2-oxopentanedial, soluble in water, suggesting the formation of different structures with various polarity than the ones observed in the D-glucose case.

4. Conclusions

Formation of heavy molecular weight compounds during the catalytic hydroconversion of pyrolysis bio-oil must be avoided for industrial upscaling. To describe those phenomena, two representative compounds were studied in a batch reactor with a NiMo/alumina reduced catalyst and tested in representative bio-oil HDC conditions.

In our operating conditions, chosen to be in accordance with the catalytic hydroconversion of a bio-oil, glucose and furfural hydroconversion were leading to numerous components in the liquid fraction. GC-FID analysis of this fraction was not sufficient to detect and quantify all the products. Thanks to SEC analysis and carbon balances the presence of heavy products was confirmed. A multi-techniques analytical strategy was set to get an insight of soluble macromolecules leading to the solid formation. Solid state ^{13}C NMR analysis of solid residues from the D-glucose conversion revealed aromatics rings which were confirmed by the FT-ICR MS of a liquid effluent. Such compounds were likely formed through equilibrated dehydration reactions. Indeed, when a high water content was present in the feed D-glucose was preserved from dehydration reactions contrarily to furfural which was prone to be hydrated into soluble macromolecules precursors.

In a following work, the catalytic hydroconversion of model compounds mixture which mimic bio-oils conversion under the same operating conditions will be presented.

Acknowledgments

Authors thanks for fruitful discussions and reviews of this paper: F. Albrieux, N. Charon, A. Le Masle and V. Souchon. In addition, M. Ozagac is grateful to F. Neyret-Martinez, L. Assam, R. Comte and S. Sivault.

Appendix A. Supplementary data

Supplementary data related to this article can be found at <http://>

dx.doi.org/10.1016/j.biombioe.2016.10.007.

References

- [1] E. Furimsky, Catalytic hydrodeoxygenation, *Appl. Catal. Gen.* 199 (2000) 147–190.
- [2] A.V. Bridgwater, Review of fast pyrolysis of biomass and product upgrading, *Biomass Bioenergy* 38 (2012) 68–94.
- [3] D.C. Elliott, Historical developments in hydroprocessing bio-oils, *Energy Fuel* 21 (2007) 1792–1815.
- [4] R.H. Venderbosch, A.R. Ardiyanti, J. Wildschut, A. Oasmaa, H.J. Heeres, Stabilization of biomass-derived pyrolysis oils, *J. Chem. Tech. Biotechnol.* 85 (2010) 674–686.
- [4] R.H. Venderbosch, H.J. Heeres, in: Marco Aurelio Dos Santos Bernardes (Ed.), *Pyrolysis Oil Stabilisation by Catalytic Hydrotreatment*, Biofuel's Engineering Process Technology, 2011.
- [6] D.C. Elliott, S.J. Lee, T.R. Hart, Stabilization of Fast Pyrolysis Oil: Post Processing, PNNL Report – 21549, 2012.
- [7] A. Oasmaa, P. Peacocke, *A Guide to Physical Property Characterisation of Biomass-derived Fast Pyrolysis Liquids. A Guide*, vol. 731, VTT Publications, 2010.
- [8] R. Bayerbach, V.D. Nguyen, U. Schurr, D. Meier, Characterization of the water-insoluble fraction from fast pyrolysis liquids (pyrolytic lignin): part III. Molar mass characteristics by SEC, MALDI-TOF-MS, LDI-TOF-MS, and Py-FIMS, *J. Anal. Appl. Pyrol.* 77 (2006) 95–101.
- [9] E. Hoekstra, S.R.A. Kersten, A. Tudos, D. Meier, K.J.A. Hogendoorn, Possibilities and pitfalls in analyzing (upgraded) pyrolysis oil by size exclusion chromatography (SEC), *J. Anal. Appl. Pyrol.* 91 (2011) 76–88.
- [10] M. Castellví Barnés, J.P. Lange, G. van Rossum, S.R.A. Kersten, A new approach for bio-oil characterization based on gel permeation chromatography preparative fractionation, *J. Anal. Appl. Pyrol.* 113 (2015) 444–453.
- [11] A. Oasmaa, E. Kuoppala, Y. Solantausta, Fast pyrolysis of forestry residue. 2. Physicochemical composition of product liquid, *Energy Fuel* 17 (2003) 433–443.
- [12] A.H. Zacher, M.V. Olarte, D.M. Santosa, D.C. Elliott, S.B. Jones, A review and perspective of recent bio-oil hydrotreating research, *Green Chem.* 16 (2014) 491–515.
- [13] E. Laurent, B. Delmon, Study of the hydrodeoxygenation of carbonyl, catalytic and guaiacyl groups over sulfided CoMo/Al₂O₃ and NiMo/Al₂O₃ catalysts: I. Catalytic reaction schemes, *Appl. Catal. Gen.* 109 (1994) 97–115.
- [14] F.-X. Collard, J. Blin, A review on pyrolysis of biomass constituents: mechanisms and composition of the products obtained from the conversion of cellulose, hemicelluloses and lignin, *Renew. Sustain. Energy Rev.* 38 (2014) 594–608.
- [15] R. Gunawan, X. Li, A. Larcher, X. Hu, D. Mourant, W. Chaiwat, H. Wu, C. Zhu Li, Hydrolysis and glycosidation of sugars during the esterification of fast pyrolysis bio-oil, *Fuel* 95 (2012) 146–151.
- [16] A.B. Bindwal, P.D. Vaidya, Kinetics of aqueous-phase hydrogenation of levoglucosan over Ru/C catalyst, *Ind. Eng. Chem. Res.* 52 (2013) 17781–17789.
- [17] T.P. Vispute, G.W. Huber, Production of hydrogen, alkanes and polyols by aqueous phase processing of wood-derived pyrolysis oils, *Green Chem.* 11 (2009) 1433–1445.
- [18] S. Helle, N.M. Bennett, K. Lau, J.H. Matsuib, S.J.B. Duffb, A kinetic model for production of glucose by hydrolysis of levoglucosan and cellobiosan from pyrolysis oil, *Carbohydr. Res.* 342 (2007) 2365–2370.
- [19] R.R. Davda, J.W. Shabaker, G.W. Huber, R.D. Cortright, J.A. Dumesic, Gaseous-phase reforming of ethylene glycol on silica-supported metal catalysts, *Appl. Catal. B Environ.* 43 (2003) 13–26.
- [20] R.D. Cortright, R.R. Davda, J.A. Dumesic, Hydrogen from catalytic reforming of biomass-derived hydrocarbons in liquid water, *Nature* 418 (2002) 964–967.
- [21] C. Rhodes, G.J. Hutchings, A.M. Ward, Water-gas shift reaction: finding the mechanistic boundary, *Catal. Today* 23 (1995) 43–58.
- [22] G.W. Huber, J.N. Chheda, C.J. Barrett, J.A. Dumesic, Production of liquid alkanes by aqueous-phase processing of biomass-derived carbohydrates, *Science* 308 (2005) 1446–1450.
- [23] R.R. Davda, J.W. Shabaker, G.W. Huber, R.D. Cortright, J.A. Dumesic, A review of catalytic issues and process conditions for renewable hydrogen and alkanes by aqueous-phase reforming of oxygenated hydrocarbons over supported metal catalysts, *Appl. Catal. B Environ.* 56 (2005) 171–186.
- [24] G.W. Huber, J.A. Dumesic, An overview of aqueous-phase catalytic processes for production of hydrogen and alkanes in a biorefinery, *Catal. Today* 111 (2006) 119–132.
- [25] B. Girisuta, L.P.B.M. Janssen, H.J. Heeres, A kinetic study on the decomposition of 5-hydroxymethylfurfural into levulinic acid, *Green Chem.* 8 (2006) 701–709.
- [26] J. Wildschut, J. Arentz, C.B. Rasrendra, R.H. Venderbosch, H.J. Heeres, Catalytic hydrotreatment of fast pyrolysis oil: model studies on reaction pathways for the carbohydrate fraction, *Environ. Progr. Sustain. Energy* 23 (2009) 450–460.
- [27] J. Buffle, *Complexation Reactions in Aqueous Systems: Analytical Approach*, Wiley & Sons Ltd./Ellis Horwood Ltd., Chichester, 1988.
- [28] D. Kleinhempel, Ein Beitrag zur Theorie des Huminstoffzustandes, *Albr. Thaer. Arch.* 14 (1970) 3.
- [29] N. Li, G.W. Huber, Aqueous-phase dehydration/hydrogenation of sorbitol: identification of the reaction pathway, *J. Catal.* 270 (2010) 48–59.

- [30] L. Vilcocq, A. Cabiac, C. Especel, E. Guillon, D. Duprez, Transformation of sorbitol to biofuels by heterogeneous catalysis: chemical and industrial considerations, *Oil Gas. Sci. Tech.* 68 (2013) 841–860.
- [31] S.K.R. Patil, C.R.F. Lund, Formation and growth of humins via aldol addition and condensation during acid-catalyzed conversion of 5-hydroxymethylfurfural, *Energy Fuel* 25 (2011) 4745–4755.
- [32] S.K.R. Patil, J. Heltzel, C.R.F. Lund, Comparison of structural features of humins formed catalytically from glucose, fructose, and 5-hydroxymethylfurfuraldehyde, *Energy Fuel* 26 (2012) 5281–5293.
- [33] X. Hu, R.J.M. Westerhof, L. Wu, D. Dong, C.Z. Li, Upgrading biomass-derived furans via acid-catalysis/hydrogenation: the remarkable difference between water and methanol as the solvent, *Green Chem.* 17 (2015) 219–224.
- [34] R. Mariscal, P. Maireles-Torres, M. Ojeda, I. Sádaba, M. López Granados, Furfural: a renewable and versatile platform molecule for the synthesis of chemicals and fuels, *Energy Environ. Sci.* 9 (2016) 1144–1189.
- [35] D.E. Resasco, S. Sitthisa, J. Faria, T. Prasomsri, M.P. Ruiz, in: D. Kubicka et, I. Kubickova (Eds.), *Heterogenous Catalysis in Biomass to Chemicals and Fuels - Chapt. 5 Furfural as Chemical Platform for Biofuel Production*, 2011.
- [36] S. Sitthisa, D.E. Resasco, Hydrodeoxygenation of furfural over supported metal catalysts: a comparative study of Cu, Pd and Ni, *Catal. Lett.* 141 (2011) 784–791.
- [37] S. Sitthisa, T. Pham, T. Prasomsri, T. Sooknoi, R.G. Mallinson, D.E. Resasco, Conversion of furfural and 2-methylpentanal on Pd/SiO₂ and Pd-Cu/SiO₂ catalysts, *J. Catal.* 280 (2011) 17–27.
- [38] S. Sitthisa, T. Sooknoi, Y. Ma, P.B. Balbuena, D.E. Resasco, Kinetics and mechanism of hydrogenation of furfural on Cu/SiO₂ catalysts, *J. Catal.* 277 (2011) 1–13.
- [39] K.J. Zeitsch, *The Chemistry and Technology of Furfural and its Many By-product*, in: *Sugar, Series 13*, Elsevier, The Netherlands, 2000, pp. 214–222.
- [40] A.V. Subrahmanyam, S. Thayumanavan, G.W. Huber, C-C bond formation reactions for biomass-derived molecules, *Chem. Sus. Chem.* 3 (2010) 1158–1161.
- [41] A. Gandini, M.N. Belgacem, *Furans in polymer chemistry*, *Progr. Polym. Sci.* 22 (1997) 1203–1379.
- [42] A. Oasmaa, J. Korhonen, E. Kuoppala, An approach for stability measurement of wood-based fast pyrolysis bio-oils, *Energy Fuel* 25 (2011) 3307–3313.
- [43] J.T. Scanlon, D.E. Willis, Calculation of flame ionization detector relative response factors using the effective carbon number concept, *J. Chromatogr. Sci.* 23 (1985) 333–340.
- [44] F. Chainet, J. Ponthus, C.-P. Lienemann, M. Courtiade, O.-F. Donard, Combining fourier transform-ion cyclotron resonance/mass spectrometry analysis and kendrick plots for silicon speciation and molecular characterization in petroleum products at trace levels, *Anal. Chem.* 84 (2012) 3998–4005.
- [45] C. Nédez, J.-P. Boitiaux, C.J. Cameron, B. Didillon, Optimization of the textural characteristics of an alumina to capture contaminants in natural gas, *Langmuir* 12 (1996) 3927–3931.
- [46] N. Charon, J. Ponthus, D. Espinat, F. Broust, G. Volle, J. Valette, D. Meier, Multi-technique characterization of fast pyrolysis oils, *J. Anal. Appl. Pyrol.* 116 (2015) 18–26.
- [47] E. Rogel, Molecular thermodynamic approach to the formation of mixed asphaltene–resin aggregates, *Energy Fuel* 22 (2008) 3922–3929.